# Flow Patterns in Two Nanorefrigerants R600a/CuO and R410A/CuO During the Boiling Process

Fernando Toapanta-Ramos[1], Elizabeth Suquillo[2] and Carlos Cornejo[3]

*Abstract* — **The present study aims to know the flow patterns in two nanorefrigerants R600a / CuO and R410A / CuO throughout the forced boiling process in horizontal square pipes. Those are obtained using the thermophysical properties of the refrigerants R600a and R410A in state liquid and vapor, as well as the properties of the CuO nanoparticles. The analysis was carried out using two methods: analytical and numerical. The analytical method was established by formulas and correlations through scientific articles and books to find an improvement in the two-phase heat transfer, under the conditions at an inlet temperature of 8 ° C and with a quality range of 0 to 1. This allowed to verify that by adding nanoparticles to the refrigerant, the transition between the flow regimes increases progressively, while the quality of the vapor decreases. For the numerical method, the different transition limits are specified in a simulation process in the Ansys Fluent CFD Software, under established design conditions, which consequently increases the general efficiency of any refrigeration system.**

*Keywords* — **Ansys Fluent; Boiling; Nanoparticles; Nano refrigerants; Simulation.**

*Resumen* — **El presente estudio tiene como propósito identificar los patrones de flujo en los nanorefrigerantes R600a/CuO y R410a/CuO durante el proceso de ebullición forzada en tuberías cuadradas horizontales. Dichos patrones se obtienen empleando las propiedades termofísicas de los refrigerantes R600a y R410A en estado líquido y de vapor, así como, también las propiedades de las nanopartículas de CuO. El análisis se lo realizó mediante dos métodos: analítico y numérico. El método analítico se estableció mediante fórmulas y correlaciones a través de artículos científicos y libros para encontrar una mejora en la transferencia de calor de dos fases. El trabajo se llevo a cabo bajo las condiciones a una temperatura de entrada de 8 °C y con un rango de calidad de 0 a 1, comprobando que al añadir nanopartículas al refrigerante la transición entre los regímenes de flujo aumenta de manera progresiva, mientras que, la calidad de vapor reduce. Para el método numérico se procedió a especificar los diferentes límites de transición en un proceso de simulación en el Software CFD Ansys Fluent, bajo condiciones establecidas de diseño, lo que en consecuencia aumenta la eficiencia general de cualquier sistema de refrigeración.**

[1] Fernando Toapanta-Ramos works at the Salesian Polytechnic University as a full professor, for the Mechanical Engineering Department, Quito-Ecuador (e-mail: ltoapanta@ups.edu.ec). ORCID number 0000-0002-0838-4702.

[2] Elizabeth Suquillo completed her master's degree in pedagogy with a mention in teaching and innovation at the Universidad Tecnológica Equinoccial, Quito-Ecuador (rsuquillo@est.ups.edu.ec). ORCID number 0000-0002-0507- 6042

[3] Carlos Cornejo completed his mechanical engineering and dedicated to practicing his profession. (ccomejoo@est.ups.edu.ec). ORCID number 0000-0001-8779-244X.

Manuscript Received: Sep 27, 2023
Revised: Nov 16, 2023
Accepted: Nov 22, 2023
DOI: https://doi.org/10.29019/enfoqueute.1006

*Palabras Clave* — **Ansys Fluent; Ebullición; Nanopartículas; Nanorefrigerantes; Simulación.**

## I. INTRODUCTION

THE boiling process using nanoparticles is one of the most critical heat transfer mechanisms, which plays a significant role in industrial sectors, such as cooling systems, power plants, and chemical reactors [1]. The industrial sector continually seeks new ways to improve the heat transfer properties of working fluids in refrigeration systems.

Nanofluid boiling is considered an important research study that offers various opportunities to explore new frontiers. However, it also comes with great challenges. For several years, some studies have been based on nanofluids for the improvement of heat transfer during the boiling process, however, the data on the boiling heat transfer coefficient and the critical heat flux have been unpredictable [2], [3], [4].

Wang et al. [5] point out that the usefulness of nanofluids in refrigeration systems is considered a potential way to optimize the energy efficiency and reliability of heating, ventilation, air conditioning and refrigeration installations (HVAC & R) and to make the use of environmentally friendly refrigerants economical.

Yin et al. [6] established a nanofluid model consisting of suspended nanoparticles for the improvement of heat transfer of boiling flow. The results reveal that both flow rate and heating temperature have an effect on the heat transfer from boiling flow to lower heating temperature. On the other hand, they obtained that, with an increase in the heating temperature, the suspended nanoparticles have much more abrupt rotational and translational movements, which can significantly improve the heat transfer of the nanofluids.

Mukthiyar et al. [7] point out that the most used refrigerant is the R410A refrigerant. This is a mixture of difluoromethane *(CH2F2)* and pentafluoro methane *(CHF2CF3),* being successfully marketed in air conditioning. On the other hand, Heredia et al. [8] mention that the refrigerant R410A has a high global warming potential (GWP) of 2 088. However, Fannon et al. [9] suggest that R410A refrigerant has better performance and minimizes pressure drop, especially for high refrigerant flow rates. Which indicates that R410A would be a better option for the design of new cooling systems direct expansion (OX).

Shao et al. [10] carried out a numerical study on the heat transfer of R410A during the boiling flow. In this study thermal phase change model in fluent was used. The results of this research show that the heat transfer coefficient increased with the mass flow growth, while it decreased with the growth of vapor quality due to the interaction of nucleate boiling and fluid convection. However, the effect of heat flux was slight on the heat

transfer coefficient of boiling flux, indicating that boiling flux is mainly governed by fluid convection.

On the other hand, Nair et al. [11] in their study of nanorefrigerants: A Comprehensive Review of its Past, Present, and Future, point out that nanorefrigerants can greatly reduce the energy consumption of a cooling system. The show that improved thermal conductivity of a nano refrigerant is only partially responsible for a higher boiling heat transfer coefficient, also show the COP of the refrigeration system increases with the addition of nanoparticles in the refrigerant. Finally, the authors mention that for the R410A refrigerant nano lubricants based on polyol oils should be used ester (POE) due to its miscibility.

Low global warming potential (GWP) refrigerants, such as R600a, have become a very important topic of study. That because they significantly reduce the emission of greenhouse gases from industries dedicated to air conditioning [12]. One example of that is the research developed by Longo et al. [13] carried out the thermodynamic and heat transfer evaluation of low-GWP refrigerants such as R600a, R1234ze (Z), and R1233zd (E) as an alternative to traditional low-pressure HFC refrigerants, such as R245fa, for heat pump (HP) and organic Rankine cycle (ORC) applications.

Gobinath and Venugopal [14] claim that CuO nanoparticles of 0.1 % volume fraction in R600a established nearly 20 % enhancement in heat transfer coefficient of the refrigerant at higher heat flux. The optimum concentration of CuO nanoparticles in stable dispersion for a prolonged time and contribute for significant enhancement in the heat transfer coefficient of R600a refrigerant is experimentally found as 0.05 % by volume.

The incorporation of solid nanoparticles into common fluids results in the formation of a nanofluid which can be considered an interesting technique to improve the thermal characteristics of a working fluid [15]. Akhavan-Behabadi et al. [16] executed an experimental study on the effect of CuO nanoparticles on the boiling flux of the mixture (R600a/oil) inside a smooth horizontal tube. These experiments were carried out under parameters of mass velocities of 50 to 400 $kg/m^2s$, inlet vapor qualities of 0 to 0.9, heat fluxes of 3 to 8 $kW/m^2$ and mass fractions of CuO nanoparticles from 0 to 1.5 % by weight. The mixing of the nanoparticles with the base fluid was carried out by passing them through a system at high speed for approximately 3 hours. The results reveal that the addition of CuO nanoparticles significantly improves heat transfer by up to 63 % relative to the heat transfer coefficient of (R600a/oil) without nanoparticles.

In the research carried out by Rabiee and Atf [17], a numerical study was carried out using computational fluid dynamics (CFO), in which AZ2O3 and CuO nanoparticles were incorporated into the fluid, basis to achieve an increase in the heat transfer coefficient during the boiling process. For this study, the Reynolds-Averaged Navier-Stokes equations were used accompanied by a mechanistic model developed by the Rensselaer Polytechnic Institute (RPI) to simulate the boiling flow field with an Eulerian-Eulerian approach for each phase. They concluded that, copper oxide compared to alumina nanoparticles would lead to higher amounts of heat transfer coefficients along pipes.

Sharif et al. [18] developed a mechanism to improve the performance of the refrigeration system through the use of nanorefrigerants and nanolubricants. This study mention that, the use of nanorefrigerants and nanolubricants in the vapor compression refrigeration system (VCRS, for its acronym in English) increased heat transfer coefficients from 12 % to 101 % and improved thermal conductivity by up to 4 %. The solubility and miscibility of the coolant-oil mixture with nanoparticle additives was improved by up to 12 % and showed a 24 % COP improvement. On the other hand, Senthilkumar [19] in their prospective study of nanolubricants and nanorefrigerants on energy savings in the vapor compression refrigeration system point out that, in the R410A refrigeration system, COPs of 4 were obtained, likewise a 8 % with 0.1 % and 0.5 % and 7 % cooling capacity using diamond nanoparticles.

Flow patterns are considered to be the configurations of a fluid that are formed when transporting two or more phases together through a pipe. These have many applications in industry, such as nuclear power plants, heat exchangers and chemical reactors [20], [21].

Lee et al. [22] conducted an investigation on the boiling flow patterns and drying characteristics of R-1234ze (E) in a plate exchanger (PHE), classifying these patterns into three flow regimes which are: rough liquid film flow, pulsating annular and stable annular flow. The boiling flow pattern map of R- 1234ze (E) in the exchanger was carried out in terms of liquid and vapor surface moments. Transitions of flow regimes on the map were expressed in terms of dimensionless numbers. Furthermore, based on the relationship between heat transfer coefficient and flow patterns in the PHE, stable annular flow was recommended as a preferable pattern to achieve very high heat transfer coefficients.

Yang et al. [23] carried out an experimental study of the flow patterns of R600a in a smooth horizontal tube with an internal diameter of 6 mm using a high-speed camera, where four main flow regimes could be observed: piston flow, corrugated- stratified, slug and annular. The experiments were carried out under conditions of saturation pressure of 0.215 to 0.415 MPa, mass fluxes of 67 to 194 $kg/m^2s$ and heat fluxes of 10.6 to 75.0 $kW/m^2$, respectively. Eight correlations were evaluated showing that the Liu and Winterton correlation provides the best fit to the experimental data with a mean absolute relative deviation of 11.5 %.

In another investigation, Copetti et al. [24] carried out an experimental study of the boiling flow of the refrigerant R600a in an aluminum tube of 1.47 mm hydraulic diameter. This study was carried out considering heat fluxes in the range of 5 to 30 $kW/m^2$, mass velocities adjusted to discrete values in the range of 50 to 200 $kg/m^2s$ and a saturation temperature of 20 °C. In addition, they presented some images of flow patterns, in different conditions, the main patterns identified were slug, intermittent and annular. The results show that the heat coefficient increases with increasing heat flux, and when the mass velocity (G) is high the growth effect is even greater.

Abdollahi et al. [25] carried out a numerical investigation to study heat transfer characteristics of nanofluids flowing through heat sink having a V-type inlet and outlet arrangement. *SiO-2 — water, AI2O3 — water, ZnO — water,* and *CuO — water* nanofluids were used as working fluids in the investigation. The average diameter size of the nanoparticles used was 30 nm, 40 nm, and 60 nm and volumetric concentration varied from 1 % to 2 %.

The objective of this research is to know and understand how the flow patterns of two highly used refrigerants are affected when they are mixed with nanoparticles.

## II. METHODS AND METHODOLOGY

Nanorefrigerants are mainly used in low temperature applications, such as air conditioning, refrigeration systems and vapor compression systems [26]. The addition of nanoparticles, especially metal oxides in the refrigerant, varies the properties and increases the heat transfer performance, improving the heat transfer performance of refrigeration systems [27].

### *A. Thermophysical Properties*

Thermophysical properties represent important parameters that are obtained using the Engineering Equation Solver (EES) software.

Therefore, the corresponding properties of the R600a refrigerant in liquid and vapor states are observed in Table I.

TABLE I
THERMOPHYSICAL PROPERTIES OF R600A REFRIGERANT [28]

| Property | Unit | Liquid | Vapor |
|---|---|---|---|
| Density | *kg/m³* | 571 | 5.507 |
| Specific heat | J/kg·K | 2 345 | 1 690 |
| Thermal conductivity | W/m·K | 0.09535 | 0.01516 |
| Viscosity | Pa·s | 1.82E-04 | 7.21E-06 |
| Enthalpy of vaporization | J/kg | 347 149 | 347 149 |

The thermodynamic properties of R410A as a zeotropic refrigerant are shown in Table II, for both the liquid and vapor phases.

TABLE II
THERMOPHYSICAL PROPERTIES OF R410A REFRIGERANT [28]

| PROPERTY | UNIT | LIQUID | VAPOR |
|---|---|---|---|
| Density | *kg/m³* | 1137 | 39.4 |
| Specific heat | J/kg·K | 1 564 | 1 209 |
| Thermal conductivity | W/m·K | 0.09857 | 0.01336 |
| Viscosity | Pa·s | 1.50E-04 | 1.18E-05 |
| Enthalpy of vaporization | J/kg | 211 258 | 211 258 |

TABLE III
PHYSICAL AND THERMAL PROPERTIES OF COPPER OXIDE [29]

| Property | Unit | Amount |
|---|---|---|
| Density | *kg/m³* | 6 400 |
| Specific heat | J/kg·K | 550.5 |
| Thermal conductivity | W/m·K | 32.9 |

### *B. Analytical Model*

To obtain the flow patterns, dimensionless variables proposed in the study carried out by Taitel-Dukler are used, which have been modified in the research by Kattan et al. [30], therefore it is necessary to define equations 1 to 6:

$$h_{LD} = \frac{h_L}{D} \tag{1}$$

$$P_{LD} = \frac{P_L}{D} \tag{2}$$

$$P_{VD} = \frac{P_V}{D} \tag{3}$$

$$P_{iD} = \frac{P_i}{D} \tag{4}$$

$$A_{VD} = \frac{A_V}{D^2} \tag{5}$$

$$A_{LD} = \frac{A_L}{D^2} \tag{6}$$

Where, $h_L$ is the height of the liquid [m], $D$ is the internal diameter of the tube [m], $P_L$ is the wet part of the perimeter[m], while, $P_v$ is the complementary part of the perimeter in contact with the vapor [m], $A_L$ and $A_v$ are the corresponding cross-sectional areas [m²]and $P_i$ is the phase interface *[m]*.

On the other hand, for the calculation of the average local void fraction from the steam quality, derived from the work carried out by Rouhani and Axelsson [31] for horizontal pipes in a section void fraction transversal, e. Equation 7.

$$\varepsilon = \frac{x}{\rho_V}[(1+0.12(1-x))(\frac{x}{\rho_V}+\frac{1-x}{\rho_L}+\frac{1.18(1-x)[g\sigma(\rho_L-\rho_V]^{0.25}}{G\rho_L^{0.5}}]^{-1} \tag{7}$$

*Where,* x is the vapor quality, *Pv* and $P_L$ are the density of the vapor and liquid respectively *[kg/m³],* g is the acceleration of gravity [m/s²], σ is the surface tension *[N/m]* and G is the total mass velocity of liquid and vapor *[kg/sm²].*

The average local void fraction model provides an explicit function of the total mass flux. Therefore, the surface section of tube A, the values of $A_{LD}$ and $A_{VD}$ are directly identifiable. Equations 8 and 9.

$$A_{VD} = \frac{A\varepsilon}{D^2} \tag{8}$$

$$A_{LD} = \frac{A-(1-\varepsilon)}{D^2} \tag{9}$$

On the other hand, the dimensions of the liquid height $h_{LD}$ and the dimensionless length of the liquid-vapor interface $P_{iD}$ can be expressed as a function of the stratified flow angle $\theta_{strat}$. Where, $_{qstrat}$ is the stratified flow angle of the tube perimeter *[rad],* it can be determined from an approximate expression, evaluated by Biberg [32]. Equation 10.

$$\theta_{strat} = 2\pi - 2\{\pi(1-\varepsilon) + (\frac{3\pi}{2})^{1/3}[1-2(1-\varepsilon) + (1-\varepsilon)^{1/3} - \varepsilon^{1/3}] - \frac{1}{200}(1-\varepsilon)\varepsilon[1-2(1-\varepsilon)][1+4((1-\varepsilon)^2+\varepsilon^2)]\} \quad (10)$$

Consequently, since the void fraction e is a function of the mass velocity G, it influences the position of the transition curves in the flow maps, proposed by Klimenko-Fyodorov [33]. Equation 11.

$$G = \frac{[(\rho_L - \rho_V)]gD^{0.5}}{\{0.074(\frac{D}{(b_{La})^{0.67}}\frac{x^2}{\rho_V} + g[1-(\frac{\rho_V}{\rho_L})^{0.1}]^2\frac{(1-x)^2}{\rho_L}\}^{0.5}} \quad (11)$$

Where, $b_{La}$ is the Laplace constant.

### C. Stratified and Intermittent/annular Flow Pattern

This flow pattern occurs at very low G mass velocities when the Kelvin-Helmholtz instability criterion is counteracted by viscous forces. It is done using the equation 12 proposed by Kattan et al. [30].

$$G_{strat} = \left\{\frac{226.3^2 A_{LD} A_{VD}^2 \rho_V(\rho_L - \rho_V)\mu_L g}{x^2(1-x)\pi^3}\right\}^{1/3} \quad (12)$$

Where, $G_{strat}$ is the stratified flow transition mass velocity *[kg/m²s]*.

The annular flow pattern is obtained when the liquid wets the entire periphery of the tube with the vapor flowing in the center of the tube [34]. The annular flow pattern has been considered to be achieved when the movement of the liquid flowing at the top of the tube [35].

The intermittent flow pattern occurs at low temperature, therefore, between intermittent and annular flow is a function of the void fraction [35]. It is defined by a fixed Martinelli parameter *X*tt = 0.34

### D. Stratified-Wavy and Drying-Fog Flow Pattern

It is characterized by a wavy interface of the liquid, where waves exist and these are of reduced magnitude and cannot reach the upper part of the tube [35].

It is calculated from the original expression of Kattan et al. [30]. Equation 13.

$$G_{wavy} = \left[\frac{16A_{VD}gD\rho_L\rho_V}{x^2\pi^2(1-(2h_{LD}-1)^2)^{0.5}}\right]^{0.5} \left[\frac{\pi^2}{25h_{LD}^2}\left(\frac{We}{Fr}\right)_L^{-1} + 1\right]^{0.5} + 50 \quad (13)$$

Where, *Gwavy* is the wave flow transition mass velocity *kg/m²s*. However, to obtain the Froude number the following expression is used. Equations 14 and 15:

$$Fr_L = \left[\frac{G^2}{\rho_L^2 gD}\right] \quad (14)$$

$$Fr_V = \left[\frac{G^2}{\rho_V^2 gD}\right] \quad (15)$$

Where, *FrL* and *FrV* is the Froude number for liquid and vapor, respectively.

Kattan et al. [36] used the following equations to find the transition limits of drying and fog flux. Equations 16 and 17.

$$G_{dryout} = \left[\frac{1}{0.235}\left(ln(\frac{0.58}{x}) + 0.52\right)\left(\frac{D}{\rho_v\sigma}\right)^{-0.17}\right]^{0.926} \left[\left(\frac{1}{gD\rho_V(\rho_L-\rho_V)}\right)^{-0.37}\left(\frac{\rho_V}{\rho_L}\right)^{-0.25}\left(\frac{q}{q_{crit}}\right)^{-0.70}\right]^{0.926} \quad (16)$$

$$G_{mist} = \left[\frac{1}{0.0058}\left(ln(\frac{0.61}{x}) + 0.57\right)\left(\frac{D}{\rho_v\sigma}\right)^{-0.38}\right]^{0.943} \left[\left(\frac{1}{gD\rho_V(\rho_L-\rho_V)}\right)^{-0.15}\left(\frac{\rho_V}{\rho_L}\right)^{-0.09}\left(\frac{q}{q_{crit}}\right)^{-0.27}\right]^{0.943} \quad (17)$$

Where, *Gdryout* is the drying transition mass velocity [*kg/m²s*], *G*mist is the fog flow transition mass velocity [*kg/m²s*] and q is the fog flux local heat [*W/m²*]. The approach of Mori et al. [37] includes the new drying limits in his research and they can be calculated from the equations 18 and 19:

$$X_{di} = 0.58e[0.52 - 0.23We_v^{-0.17}Fr_V^{0.37}\left(\frac{\rho_V}{\rho_L}\right)^{0.25}\left(\frac{q}{q_{crit}}\right)^{0.7}] \quad (18)$$

$$X_{de} = 0.61e[0.57 - 5.8x10^{-3}We_v^{0.38}Fr_V^{0.15}\left(\frac{\rho_V}{\rho_L}\right)^{-0.09}\left(\frac{q}{q_{crit}}\right)^{0.27}] \quad (19)$$

Therefore, to calculate the critical heat flux *q*crit [*kg/m²s*] the expression, given by Kutateladze [38] is used. Equations 20.

$$q_{crit} = 0.131\rho_V^{0.5}h_{LV}\left(g(\rho_L-\rho_V)\sigma\right)^{0.25} \quad (20)$$

### E. Numerical Model

ANSYS CFD is a tool that offers higher accuracy quantitative forecasts of fluid interactions and connections [39].

The pipes are manufactured to transport fluids inside, so for this study a square horizontal pipe is used, whose design parameters are shown in Table IV.

For this purpose, within the Fluent setup, the materials and edge conditions are configured for correct operation. Below, Table V shows the simulation parameters.

The volume fractions for both liquid and vapor phases are defined by the equation 21:

$$V_q = \int_V \varphi_q dV \tag{21}$$

Where, the volume divisions refer to the space involved in each phase, and the laws of conservation of mass and moment are fulfilled in each stage exclusively [39].

TABLE IV
DESIGN PARAMETERS OF SQUARE PIPE

| Parameter | Value | Unit |
|---|---|---|
| Hydraulic diameter (Dh) | 0.01 | m |
| Length (L) | 2 | m |
| Thickness (e) | 0.5 | mm |
| Material | Copper | |

TABLE V
PARAMETERS USED IN THE SIMULATION

| Parameter | Numeric value |
|---|---|
| Mass speed ($kg/m^2s$) | 100 and 300 |
| Heat flux ($W/m^2$) | 10 000 and 20 000 |
| Saturation temperature (°C) | 8 |
| CuO nanoparticle concentration (%) | 3 and 5 |

Equation of conservation of mass or also called the equation of continuity, this defines the increase and decrease of mass that occurs in the phase change (liquid-vapor) taking into account the principle of conservation of mass. Equation 22.

$$\frac{\partial}{\partial_t}(\alpha_q \rho_q) + \nabla(\alpha_q \rho_q V_q) = \sum_{p=1}^{n}(m_{pq} m_{qp}) + S_q \tag{22}$$

Equation 23 for this balance shows the external forces acting within a phase change, which correspond to the movement of the mass, which are produced due to fluid turbulence. Equation 23.

$$\frac{\partial}{\partial_t}(\alpha_q \rho_q \overrightarrow{V_q}) + \nabla(\alpha_q \rho_q \overrightarrow{V_q}) = -\alpha_q \nabla_p + \nabla \overline{\overline{t_q}} + \alpha_q \rho_q \vec{g} \tag{23}$$

### *F. Mesh Generation*

The geometry mesh is implemented for assigning the boundary conditions, using a body size of 1.5 mm, as can be seen in Figure 1.

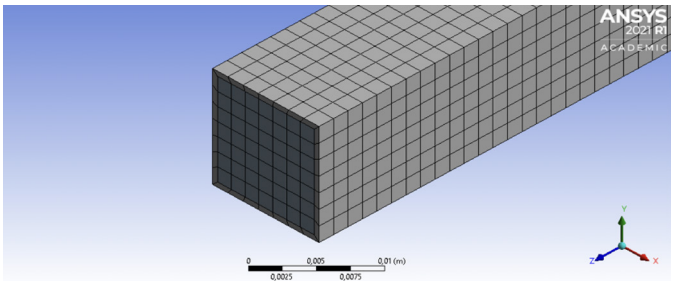


**Fig. 1.** Geometry meshing.

Obtaining its quality using the Skewnees tool within Fluent's metric meshing, the same as seen in Figure 2, this type of quality states that as long as the number of elements and nodes is located in a range of 0 to 0.5, the meshing will converge from successful way.

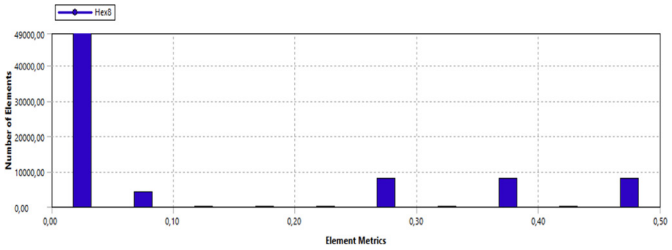


**Fig. 2.** Mesh quality.

## III. RESULTS AND DISCUSSION

The flow maps of R600a refrigerant are compared with the research of Yang et al. [23] who studies pure flow maps. The flow maps for R600a/CuO upon adding 3 % and 5 % nanoparticles in concentration as shown in Figure 3 a) and b), the dimensions of diameter, mass velocity and heat flux are kept constant. Furthermore, it can be seen that the slug/stratified-wavy flow regime zone is more extensive, since the transition fine between slug and slug+SW has a higher mass velocity.

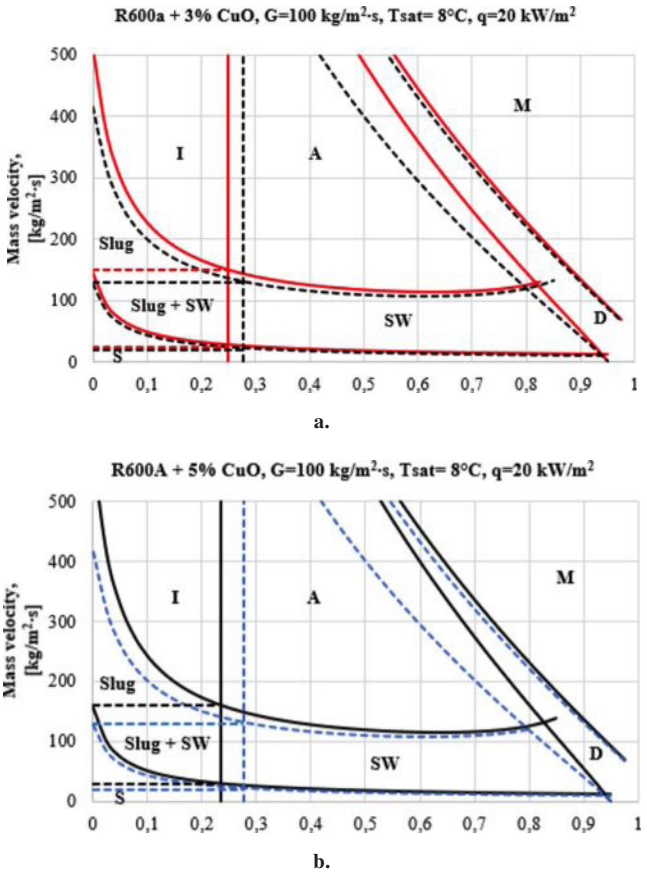


**Fig. 3. a)** Flow map for pure R600a refrigerant and R600a + 3 % CuO and **b)** Flow map for pure R600a refrigerant and R600a + 5 % CuO.

To check the accuracy of the flowchart, it is compared with the work of Hu et al. [40] who carried out a study of the flow diagrams of pure R410A refrigerant and R410A containing lubricating oil. In Figure 4 a) and b), the comparison of the flow maps for pure R410A and R410A with 3 % and 5 % nanoparticles, in which it is possible to see that the vapor quality is lower at the flow interface ( I/A), however, this is directed to the left, thus accelerating the phase change process, because, when adding nanoparticles, the quality varies by 10 %, and reaching the drying regime is faster than for the pure refrigerant, in the same way as for the fog zone.

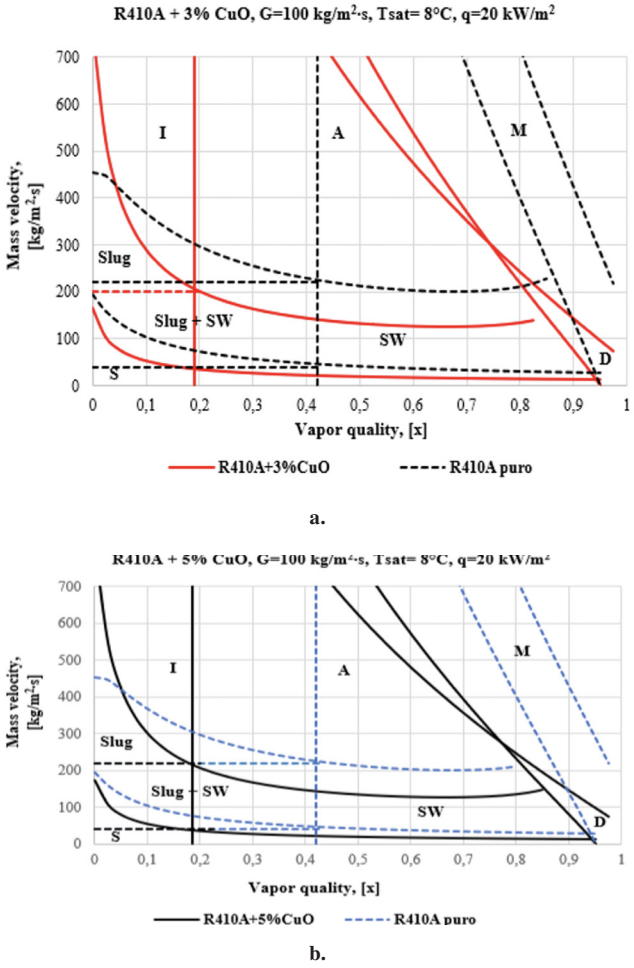


**Fig. 4. a)** Flow map for pure R410A refrigerant and R410A + 3 % CuO and **b)** Flow map for pure R410A refrigerant and R410A + 5 % CuO.

Figure 5 indicates that the flow maps for R600a/CuO with 3 % nanoparticles, the transition line between slug and slug+SW has a higher mass velocity. While, by adding 5 % of nanoparticles, a greater heat transfer occurs, causing an intersection between the zones of the annular intermittent flow.

Figure 6 shows the simulation results for the R410A refrigerant with a mixture of CuO nanoparticles, where the heat transfer is dominated by subcooled boiling and nucleated boiling, which is why the phase change when adding a 3 % and 5 % CuO nanoparticles are produced at lower vapor qualities, thus generating the transition limit (I/A) to develop early in the boiling process.

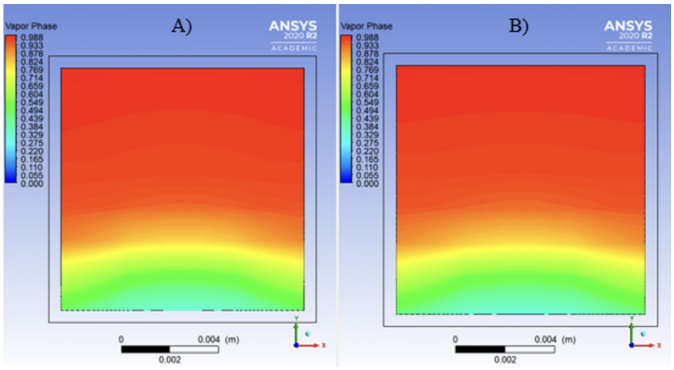


**Fig. 5.** Contour of the vapor volume fraction distribution for the R600a/CuO nanorefrigerant with G= 100 $kg/m^2s$ and q= 20 $kW/m^2$ for A) R600a + 3 % CuO, B) R600a + 5 % CuO.

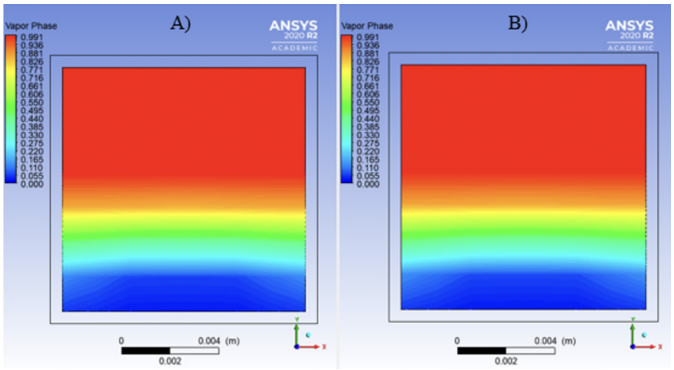


**Fig. 6.** Contour of the vapor volume fraction distribution for the R410A/CuO nanorefrigerant with G= 100 $kg/m^2s$ and q= 20 $kW/m^2$ for A) R410A + 3 % CuO, B) R410A + 5 % CuO.

## IV. CONCLUSIONS

The following conclusions are drawn by studying the flow patterns in R600a and R410A refrigerants in pure state and with nanoparticles:

- Through an analytical study, it was proven that by adding nanoparticles in concentrations of 3 % to 5 % to the R600a and R410A refrigerants, the transition between the flow regimes increases by 25 %, while the vapor quality is reduced. For this reason it is deduced that its heat transfer increases and the phase change process begins to occur at short lengths within the pipe.
- In the numerical study carried out it was concluded that in the R600a refrigerant the flow boiling heat transfer coefficient increased from 4500 to 5400 $kg/m^2s$ using CuO nanoparticles. Also the heat transfer coefficient was improved in regimes such as slug and stratified-wavy (SW). That occur at vapor qualities between 0.1 to 0.5 and as its quality increased this coefficient decreased from 3600 to 2400 $kg/m^2s$. The result is drying (D) and fog (M) regimes occupying a vapor volume of less than 20 %.
- Through an analytical and numerical study, the flow boiling heat transfer performance of CuO nanoparticles in the refrigerants R600a and R410A was analyzed.

## V. ACKNOWLEDGMENT

The authors thank the Salesian Polytechnic University and for the research group Research Group in Engineering, Productivity and Industrial Simulation (GUPSI) and the ASHRAE-UPS Branch group for the technical and administrative support provided to the development of this studio.

## REFERENCES

[1] M. Goodarzi, I. Tlili, H. Moria, T. A. Alkanhal, R. Ellahi, A. E. Anqi, and M. R. Safaei, "Boiling heat transfer characteristics of graphene oxide nanoplatelets nano-suspensions of water-perfluorohexane (c6fl4) and water-n-pentane," *Alexandria Engineering Journal*, vol. 59, no. 6, pp. 4511-4521, 2020.

[2] A. Khan and H. M. Ali, "A comprehensive review on pool boiling heat transfer using nanofluids," *Thermal Science,* vol. 23, no. 5 Part B, pp. 3209-3237, 2019.

[3] S. Vafaei, "Nanofluid pool boiling heat transfer phenomenon," *Powder Technology,* vol. 277, pp. 181-192, 2015.

[4] A. Redhwan, W. Azmi, M. Sharif, and R. Mamat, "Development of nanorefrigerants for various types of refrigerant based: A comprehensive review on performance," *International Communications in Heat and Mass Transfer,* vol. 76, pp. 285-293, 2016.

[5] R. Wang, Q. Wu, and Y. Wu, "Use of nanoparticles to make mineral oil lubricants feasible for use in a residential air conditioner employing hydro-fluorocarbons refrigerants," *Energy and Buildings,* vol. 42, no. 11, pp. 2111-2117, 2010.

[6] X. Yin, C. Hu, M. Bai, and J. Lv, "An investigation on the heat transfer characteristics of nanofluids in flow boiling by molecular dynamics simulations," *International Journal of Heat and Mass Transfer,* vol. 162, p. 120338, 2020.

[7] S. Mukthiyar, D. R. Sarath, B. V. Kumar, and A. Madabhushi, "Design and cfd analysis of r410a refrigerant in convergent nozzle," *Materials Today: Proceedings,* vol. 5, no. 9, pp. 19463-19470, 2018.

[8] Y. Heredia-Aricapa, J. Behnan-Flores, A. Mota-Babiloni, J. Serrano-Arellano, and J. J. García-Pabón, "Overview of low gwp mixtures for the replacement of hfc refrigerants: R134a, r404a and r410a," *International Journal of Refrigeration,* vol. Ill, pp. 113-123, 2020.

[9] J.-L. C. Fannou, C. Rousseau, L. Lamarche, and S. Kajl, "A comparative performance study of a direct expansion geothermal evaporator using r410a and r407c as refrigerant alternatives to r22," *Applied Thermal Engineering,* vol. 82, pp. 306-317, 2015.

[10] Y. Shao, S. Deng, P. Lu, D. Zhao, L. Zhao, W. Su, and M. Ma, "A numerical study on heat transfer of r410a during flow boiling," *Energy Procedía,* vol. 158, pp. 5414-5420, 2019.

[11] V. Nair, P. Tailor, and A. Parekh, "Nanorefrigerants: A comprehensive review on its past, present and future," *International journal of refrigeration,* vol. 67, pp. 290-307, 2016.

[12] Y. Sun, J. Wang, and Y. Hu, "Effect of refrigerant/oil solubility on thermodynamic performance of the evaporator working with r600a and dme," *The Journal of Chemical Thermodynamics,* vol. 154, p. 106331, 2021.

[13] G. A. Longo, S. Mancin, G. Righetti, C. Zilio, and J. S. Brown, "Assessment of the low-gwp refrigerants r600a, rl234ze (z) and rl233zd (e) for heat pump and organic rankine cycle applications," *Applied Thermal Engineering,* vol. 167, p. 114804, 2020.

[14] N. Gobinath and T. Venugopal, "Nucleate pool boiling heat transfer characteristics of r600a with cuo nanoparticles," *Journal of Mechanical Science and Technology,* vol. 33, pp. 465-473, 2019.

[15] A. Shafee, B. Rezaeianjouybari, M. Sheikholeslami, M. Allahyari, and H. Babazadeh, "Boiling process with incorporating nanoparticles through a flattened channel using experimental approach," *Journal of Thermal Analysis and Calorimetry,* vol. 143, pp. 3569-3576, 2021.

[16] M. Akhavan-Behabadi, M. Nasr, and S. Baqeri, "Experimental investigation of flow boiling heat transfer of r-600a/oil/cuo in a plain horizontal tube," *Experimental Thermal and Fluid Science,* vol. 58, pp. 105-111, 2014.

[17] A. Rabiee and A. Atf, "A computational fluid dynamics investigation of various nanofluids in a boiling flow field," *Progress in Nuclear Energy,* vol. 95, pp. 61-69, 2017.

[18] M. Sharif, W. Azmi, R. Mamat, and A. Shaiful, "Mechanism for improvement in refrigeration system performance by using nanorefrigerants and nanolubricants-a review," *International Communications in Heat and Mass Transfer,* vol. 92, pp. 56-63, 2018.

[19] A. Senthilkumar, A. Anderson, and R. Braveen, "Prospective of nanolubricants and nano refrigerants on energy saving in vapour compression refrigeration system-a review," *Materials Today: Proceedings,* vol. 33, pp. 886-889, 2020.

[20] E. Costa-Patry and J. R. Thome, "Flow pattern-based flow boiling heat transfer model for microchannels," *International Journal of Refrigeration,* vol. 36, no. 2, pp. 414-420, 2013.

[21] S. Mimouni, S. Fleau, and S. Vincent, "Cfd calculations of flow pattern maps and les of multiphase flows," *Nuclear Engineering and Design,* vol. 321, pp. 118-131, 2017.

[22] D. Lee, C. Jo, B. Kim, and Y. Kim, "Boiling flow patterns and dry-out characteristics of r-1234ze (e) in a plate heat exchanger," *International Journal of Heat and Mass Transfer,* vol. 161, p. 120308, 2020.

[23] Z. Yang, M. Gong, G. Chen, X. Zou, and J. Shen, "Two-phase flow patterns, heat transfer and pressure drop characteristics of r600a during flow boiling inside a horizontal tube," *Applied Thermal Engineering,* vol. 120, pp. 654-671, 2017.

[24] J. B. Copetti, B. de Sá Bekerle, M. H. Macagnan, J. C. Passos, and J. D. Oliveira, "Flow boiling heat transfer characteristics of r600a in multiport minichannel," *Heat Transfer Engineering,* vol. 38, no. 3, pp. 323-331, 2017.

[25] A. Abdollahi, H. Mohammed, S. M. Vanaki, A. Osia, and M. G. Haghighi, "Fluid flow and heat transfer of nanofluids in microchannel heat sink with v-type inlet/outlet arrangement," *Alexandria Engineering Journal,* vol. 56, no. 1, pp. 161-170, 2017.

[26] S. Sanukrishna, M. Murukan, and P. M. Jose, "An overview of experimental studies on nanorefrigerants: Recent research, development and applications," *International Journal of refrigeration,* vol. 88, pp. 552-577, 2018.

[27] L. Cheng and L. Liu, "Boiling and two-phase flow phenomena of refrigerant-based nanofluids: fundamentals, applications and challenges," *International journal of refrigeration,* vol. 36, no. 2, pp. 421-446, 2013.

[28] F.-C. Software, "Engineering equation solver (ees)," 2015.

[29] Q. Peng, L. Jia, C. Dang, X. Zhang, and Q. Huang, "Experimental investigation on flow condensation of rl41b with cuo nanoparticles in a vertical circular tube," *Applied Thermal Engineering,* vol. 129, pp. 812-821,2018.

[30] N. Kattan, J. Thome, and D. Favrat, "Flow boiling in horizontal tubes: part 1—development of a diabatic two-phase flow pattern map," 1998.

[31] S. Z. Rouhani and E. Axelsson, "Calculation of void volume fraction in the subcooled and quality boiling regions," *International Journal of Heat and Mass Transfer,* vol. 13, no. 2, pp. 383-393, 1970.

[32] D. Biberg, "An explicit approximation for the wetted angle in two-phase stratified pipe flow," *The Canadian Journal of Chemical Engineering,* vol. 77, no. 6, pp. 1221-1224, 1999.

[33] V. Klimenko and M. Fyodorov, "Prediction of heat transfer for two-phase forced flow in channels of different orientation," in *International Heat Transfer Conference Digital Library.* Begel House Inc., 1990.

[34] C. Park and P. Hmjak, "Co2 and r410a flow boiling heat transfer, pressure drop, and flow pattern at low temperatures in a horizontal smooth tube," *International Journal of Refrigeration,* vol. 30, no. 1, pp. 166-178, 2007.

[35] O. Zürcher, D. Favrat, and J. Thome, "Development of a diabatic two-phase flow pattern map for horizontal flow boiling," *International Journal of Heat and Mass Transfer,* vol. 45, no. 2, pp. 291-301, 2002.

[36] N. Kattan, J. R. Thome, and D. Favrat, "Flow boiling in horizontal tubes: part 3—development of a new heat transfer model based on flow pattern," 1998.

[37] H. MORI, S. YOSHIDA, K. OHISHI, and Y. KAKIMOTO, "Dryout quality and post-dryout heat transfer coefficient in horizontal evaporator tubes," in *3rd European thermal sciences conference (Heidelberg, 10-13 September 2000),* 2000, pp. 839-844.

[38] S. Kutateladze, "On the transition to film boiling under natural convection," *Kotloturbostroenie,* vol. 3, p. 10, 1948.

[39] I. ANSYS, *ANSYS FLUENT User ' s Guide,* 2021.

[40] H. Hu, G. Ding, W. Wei, Z. Wang, and K. Wang, "Heat transfer characteristics of r410a-oil mixture flow boiling inside a 7 mm straight smooth tube," *Experimental Thermal and Fluid Science,* vol. 32, no. 3, pp. 857-869, 2008.